N73-16776

NASA TECHNICAL NOTE

NASA TN D-7128

NASA TN D-7128

CASE FILE COPY

EFFECT OF A REDUCTION IN BLADE THICKNESS ON PERFORMANCE OF A SINGLE-STAGE 20.32-CENTIMETER MEAN-DIAMETER TURBINE

by William J. Nusbaum and Milton G. Kofskey

Lewis Research Center

Cleveland, Ohio 44135

NATIONAL AERONAUTICS AND SPACE ADMINISTRATION • WASHINGTON, D. C. • FEBRUARY 1973

1. Report No.	2. Government Accession No.	3. Recipient's Catalog No.
NASA TN D-7128		

4. Title and Subtitle EFFECT OF A REDUCTION IN BLADE THICKNESS ON PERFORMANCE OF A SINGLE-STAGE 20.32-CENTIMETER MEAN-DIAMETER TURBINE	5. Report Date February 1973
	6. Performing Organization Code
7. Author(s) William J. Nusbaum and Milton G. Kofskey	8. Performing Organization Report No. E-7029
	10. Work Unit No. 501-24
9. Performing Organization Name and Address Lewis Research Center National Aeronautics and Space Administration Cleveland, Ohio 44135	11. Contract or Grant No.
	13. Type of Report and Period Covered Technical Note
12. Sponsoring Agency Name and Address National Aeronautics and Space Administration Washington, D.C. 20546	14. Sponsoring Agency Code

15. Supplementary Notes

16. Abstract

As part of a program to reduce the manufacturing costs of a small gas-turbine engine, the turbine blading was reduced in thickness to facilitate coining. Tests were made to determine the effect of this modification on turbine performance. The working fluid was air at nominal inlet total conditions of 297.2 K (535° F) and 13.8 N/cm^2 (20.0 psia). Performance results are presented and compared for four stator-rotor combinations in terms of equivalent torque, mass flow, and efficiency at equivalent design speed and at inlet-total to exit-static pressure ratios of 1.8 to 3.8.

17. Key Words (Suggested by Author(s))	18. Distribution Statement
Axial flow turbine; Efficiency; Single stage turbine; Performance tests; Gas turbine	Unclassified - unlimited

19. Security Classif. (of this report)	20. Security Classif. (of this page)	21. No. of Pages	22. Price*
Unclassified	Unclassified	25	$3.00

* For sale by the National Technical Information Service, Springfield, Virginia 22151

EFFECT OF A REDUCTION IN BLADE THICKNESS ON PERFORMANCE OF A SINGLE-STAGE 20.32-CENTIMETER MEAN-DIAMETER TURBINE

by William J. Nusbaum and Milton G. Kofskey

Lewis Research Center

SUMMARY

Modifications and tests were made on the blading of the first stage of a two-stage, 20.32-centimeter (8.00-in.) mean diameter, axial-flow turbine designed for a small, low-cost turbofan engine. Results of studies indicated a substantial reduction in cost and manufacturing time if the turbine blades were coined. Therefore, both stator and rotor blades were reduced in thickness to simulate profiles that could be coined more easily. The pressure surfaces of the blades were modified to give near uniform blade thickness from leading to trailing edge. The diameter of the blade leading edge was chosen as the value of maximum thickness. First-stage performance results are presented for operation with the four possible combinations of original and modified stator and rotor blades. The working fluid was air at nominal inlet total conditions of 297.2 K (535° R) and 13.8 newtons per square centimeter (20.0 psia). Data were obtained at equivalent design speed and over a range of inlet-total to exit-static pressure ratios from 1.8 to 3.8.

Modification of the blading had little effect on the performance of the first stage. Total efficiency increased from 0.93 to 0.94 when the thin stator blades were used with either the thin or original rotor. The static efficiency also increased from 0.80 to 0.81 when the thin stator blades were used instead of the original blades.

The mass flow for the four configurations did not differ by more than 1.0 percent at any pressure ratio. The equivalent mass flow for the original first stage stator and rotor was 2.00 kilograms per second (4.41 lb/sec) at equivalent design speed and pressure ratio.

INTRODUCTION

Gas turbine engines are very attractive for use in light aircraft because of their small size and weight. At the present time, however, the high cost of these engines greatly restricts their use. The Lewis Research Center is currently conducting studies of methods for reducing the manufacturing costs of the small gas turbine engine. Reference 1 presents a description of the work being done. Results of the studies indicated a substantial reduction in cost and manufacturing time if the blades for the turbine were coined instead of machined. The coining process would be simplified if the blades were of near uniform thickness from leading to trailing edge. The question arises as to the effect on turbine performance of the change in blade profile and loading distribution when the conventional blade is replaced by a blade having near uniform thickness from leading to trailing edge.

In order to determine the effect of the change in blade profile and loading distribution on turbine performance, the first stage of the turbine of reference 2 was modified and used for this investigation. The stator and rotor blades were made with suction-surface profiles identical to those of reference 2. The pressure surfaces of both stator and rotor blades were modified to give a maximum blade thickness equal to the leading-edge diameter. This thickness was tapered to blend into the trailing edge. In order to eliminate the effect of differences in surface finish on turbine performance, the modified blades were machined to the same surface finish as the conventional blades.

Turbine tests were conducted on single-stage units under the same operating conditions and over the same range of pressure ratios (at equivalent design speed) as those used in the first-stage investigation reported in reference 2. Turbine performance was first determined with the modified rotor in combination with the original stator. The modified stator was then used in combination with the original rotor. Finally, both modified blade rows were tested together.

This report presents a brief description of the blade modification, blade loading diagrams, and the performance results obtained in the three series of tests. Comparison is made with the data presented in reference 2 for first-stage operation using both original blade rows. Test results are presented in terms of equivalent torque, mass flow, and efficiency. The report also includes the results of a radial survey of rotor exit total pressure and flow angle.

SYMBOLS

A area, cm^2; $in.^2$

Dp pressure-surface diffusion parameter, $\dfrac{(\text{blade inlet relative velocity})^2}{(\text{minimum pressure-surface velocity})^2}$

Ds suction-surface diffusion parameter, $\dfrac{(\text{maximum suction-surface velocity})^2}{(\text{blade outlet relative velocity})^2}$

g dimensional constant, SI = 1.0; 32.174 ft/sec^2

Δh specific work, joules/gram; Btu/lb

J mechanical equivalent of heat, SI = 1.0; 778.2 ft-lb/Btu

N turbine speed, rpm

p pressure, newtons/cm^2; psia

R gas constant, joules/(kg)(K); ft-lb/(lb)($^\circ$R)

R_x reaction, $\dfrac{(\text{blade outlet velocity})^2 - (\text{blade inlet velocity})^2}{(\text{blade outlet velocity})^2}$

r radius, m; ft

T absolute temperature, K; $^\circ$R

U blade velocity, m/sec; ft/sec

V absolute gas velocity, m/sec; ft/sec

V_j ideal jet speed corresponding to total- to static-pressure ratio across turbine, m/sec; ft/sec

W relative gas velocity, m/sec; ft/sec

w mass flow, kg/sec; lb/sec

α absolute gas flow angle measured from axial direction, deg

γ ratio of specific heats

δ ratio of inlet total pressure to U.S. standard sea-level pressure, p_1'/p^*

ϵ function of γ used in relating parameters to those using air inlet conditions at U.S. standard sea-level conditions, $(0.740/\gamma)[(\gamma + 1)/2]^{\gamma/\gamma-1}$

η_s static efficiency (based on inlet-total- to exit-static-pressure ratio)

η_t total efficiency (based on inlet-total- to exit-total-pressure ratio)

θ_{cr} squared ratio of critical velocity at turbine inlet to critical velocity at U.S. standard sea-level air, $(V_{cr}/V_{cr}^*)^2$

λ work-speed parameter $U_m^2/gJ\Delta h$

ν blade-jet speed ratio, U_m/V_j

τ torque, N-m: ft-lb

Subscripts:

cr condition corresponding to Mach 1

m mean radius

w outer wall

1 station at turbine inlet

2 station at stator exit

3 station at rotor exit

Superscripts:

' absolute total state

* U.S. standard sea-level conditions (temperature, 288.15 K (518.67° R); pressure, 10.13 N/cm^2 (14.70 psia))

TURBINE DESIGN

Design Requirements and Velocity Diagrams

The turbine used for the investigation had the same design requirements as those of the first stage of a two-stage axial flow turbine that was designed for a small, low-cost turbofan engine. Design information as well as performance results of this 20.32-centimeter (8.00-in.) mean diameter turbine are given in reference 2. The design requirements for the first stage (subject turbine) are given in table I The work-speed parameter value of 0.582 is conducive to good aerodynamic efficiency because turbine work or blade loading is not excessive with respect to the mean blade speed.

The free-stream velocity diagrams for the first stage are shown in figure 1. These diagrams were computed to meet the design requirements and are based on the following assumptions:

(1) A stator total pressure loss of 4.0 percent of inlet-total pressure. This value was chosen because stator losses are generally from 3 to 4 percent of the inlet-total pressure.

(2) A total efficiency of 0.87. This value was based on material presented in reference 3, which shows efficiency as a function of the work-speed parameter λ.

(3) A constant mean diameter of 20.32 centimeters (8.00 in.).

(4) Free vortex flow.

Figure 1 shows that all velocities are subsonic with near sonic conditions existing at the exit of the stator at the hub. The relative velocity increases through the rotor, which results in a reaction that is conducive to good efficiency. There was 91.2° of turning through the rotor at the mean section. The figure also shows that there was a substantial amount of negative rotor exit whirl at all sections. This exit whirl was recoverable when operated with the second stage.

Stator Blades

The original stator blade row was designed to satisfy the velocity diagrams. The selection of the blade number of 35 was based on the results of an optimum solidity study reported in reference 4. The blade solidity at the hub, mean, and tip sections were 1.35, 1.43, and 1.39, respectively. The stator had a constant blade height of 3.363 centimeters (1.324 in.).

For this investigation the blade thickness was reduced to simulate a blade profile that could be coined more easily. The reduction of blade thickness was accomplished by changing the pressure surface. Maximum blade thickness was set equal to the leading-edge diameter, and the thickness was tapered to blend into the trailing edge. This method was selected because the throat dimension would be unchanged. Since the original blades were machined, the thin blades were also machined instead of coined in order to eliminate any possible effect of blade surface finish on performance.

Figure 2 shows the comparison of the original and thin stator blade profiles. Note the substantial reduction in thickness for all three blade sections. Inspection of the thin stator flow passages shows that there was no abrupt change in flow area and that the flow passage width was converging satisfactorily.

Figure 3 shows the calculated blade-surface velocities for both stator configurations for the hub, mean, and tip sections. The blade surface velocities were calculated by the computer program described in reference 5. The results of the computer program include velocities on the blade surface and throughout the passage. The transonic solution is obtained by a velocity-gradient method using information obtained from a finite-difference stream-function solution at a reduced mass flow. The trends of the suction- and pressure-surface velocities were very similar for both configurations (see fig. 3). The velocity level was noticeably lower for the thin-blade configuration and was primarily a result of the larger passage width, with the exception of the throat or minimum area. Table II, which lists the aerodynamic parameters, shows that the suction-surface diffusion was the same for both stator configurations at all three blade sections. The pressure-surface diffusion for the thin blade design is considerably larger than that for the original stator configuration. It is felt that the higher pressure-surface diffusion near the leading edge will not have any large detrimental effect on turbine performance because of the large acceleration of the flow over the remainder of the pressure surface (fig. 3). Also, a flow separation on the pressure surface will tend to shift the loading diagram closer to the original diagram. The larger acceleration that follows the large pressure-surface diffusion will mitigate any increase in losses. Therefore, there is no reason for the performance of the thin stator blade design to be significantly different from that of the original design.

Rotor Blades

The procedure used in the design of the stator blades was also used for the original rotor blade design. There were 42 blades with a solidity of 1.71 at the mean section. The inner and outer walls diverge equally with the average blade height being 3.66 centimeter (1.44 in.).

The original rotor blade shape was also altered so that the maximum thickness was equal to the leading-edge diameter. Figure 4 shows the rotor-blade profiles and passages for both rotor configurations investigated. The channel width formed by the thin blade profiles at the hub and mean section diverges and then converges.

Figure 5 shows the calculated blade surface velocities for both rotor configurations. The main difference between rotor configurations is the level of the surface velocities. The suction-surface velocities are noticeably lower for the thin blade at the hub and mean sections. Pressure-surface velocities are noticeably lower for the thin blade at all three sections than the surface velocities obtained with the original blade. Table II, which lists the diffusion values, shows that the suction-surface diffusion was the same for both rotor configurations at all three blade sections. The pressure-surface diffusion, however, was considerably larger for the thin blade than that obtained with the original rotor configuration. Using the same reasoning as used for the stator, there is no reason for any significant difference in performance for the thin rotor blade design.

All other aerodynamic parameters listed in table II were the same for the four configurations with the exception of the rotor blade tip clearance. Tip clearance was 0.030 and 0.025 centimeter (0.012 and 0.010 in.) for the original and thin blade configurations, respectively. The difference in tip clearance was due to fabrication.

Table III gives the stator- and rotor-blade coordinates for both original and thin blade profiles. A photograph of both rotor-blade configurations is shown in figure 6.

APPARATUS, INSTRUMENTATION, AND PROCEDURE

Apparatus

The apparatus (described in ref. 2) consisted of the turbine, a cradled gearbox, and a cradled dynamometer to absorb the power output of the turbine and to control turbine speed. In addition, there was inlet and exhaust piping with flow controls for setting turbine-inlet and exit pressures. The arrangement of the apparatus is shown schematically in figure 7. High-pressure dry air was supplied from the laboratory air system. The air passed through a filter, through a mass-flow measuring station consisting of a calibrated flat-plate orifice, through a remotely controlled turbine-inlet valve, through an inlet plenum, and into the turbine. After going through the turbine, the air was exhausted through a system of piping and a remotely operated valve into the laboratory low-pressure exhaust system. A 300-horsepower dynamometer cradled on trunion ball bearings was used to absorb the turbine power. The dynamometer was coupled to the turbine shafting through a gearbox cradled on hydrostatic bearings. Figure 8 shows the turbine test apparatus. Steam was injected into the exhaust downstream of the turbine in order to keep the exhaust above freezing to protect a hydraulically operated isolation valve.

Instrumentation

A torque arm attached to the dynamometer transmitted the turbine torque to a commercial strain-gage load cell.

Turbine performance was determined by measurements taken at the stator inlet and at the rotor exit. The following instrumentation at the turbine inlet (station 1) was located approximately one chord length upstream of the stator blades: three static-pressure taps equally spaced circumferentially at both hub and tip, and three total-temperature rakes each containing three thermocouples. There were three tip static-pressure taps equally spaced in a plane just downstream of the stator trailing edge (station 2). Station 3, located approximately one axial chord length downstream of the rotor exit, had the following instrumentation: six static-pressure taps equally spaced circumferentially (three each at the inner and outer walls) and a self-alining probe for flow angle, total-temperature, and total-pressure measurements. There were also five total-temperature rakes, each containing three thermocouples, at a downstream station about 50.8 centimeters (20.0 in.) from the rotor trailing edge. In the calculation of pressure ratio across the turbine, the pressure at station 3 was determined from the average of the static pressures at the inner and outer walls. The values of the pressures at the various stations were measured by unbonded type strain-gage transducers.

Procedure

Data were obtained at nominal inlet total conditions of 297.2 K (535° R) and 13.8 newtons per square centimeter (20.0 psia). Data were obtained over a range of inlet-total- to exit-static-pressure ratios from 1.8 to 3.8 at equivalent design speed.

In order to minimize the error due to a change in torque calibration from day to day, the torque calibration was obtained before and after each series of runs. Accuracy of torque measurement (as stated in ref. 2) is ±0.5 percent of the value obtained at equivalent design conditions.

The turbine was rated on the basis of both total and static efficiency. The total pressures were calculated from mass flow, static pressure, total temperature, and flow angle from the following equation:

$$p' = p\left\{\frac{1}{2} + \frac{1}{2}\left[1 + \frac{2(\gamma-1)}{\gamma}\,\frac{R}{g}\left(\frac{w\sqrt{T'}}{pA\cos\alpha}\right)^2\right]^{1/2}\right\}^{\gamma/(\gamma-1)}$$

In the calculation of turbine-inlet total pressure, the flow angle was assumed to be zero.

RESULTS AND DISCUSSION

Performance results are presented for a 20.32-centimeter (8.00-in.) mean diameter, single-stage turbine operating at the equivalent design speed of 15 336 rpm. A comparison is made between results obtained with the four possible combinations of original and thin stator blades with the original and thin rotor blades. The first section of the discussion includes the overall performance in terms of equivalent torque, equivalent mass flow, and efficiency. A second section presents the internal flow characteristics as determined from the measured static-pressure variation through the turbine and the rotor-exit radial survey of flow angle and total pressure.

Overall Performance

Turbine torque output (at equivalent design speed) is shown in figure 9 as a function of turbine pressure ratio for each of the four stator-rotor combinations. The thin-stator - thin-rotor combination appears to be slightly better than the other three. However, the difference in torque among the four configurations is less than 2 percent at all pressure ratios covered in the investigation.

Values of measured mass flow for each of the four blade configurations are plotted in figure 10. Equivalent mass flow is shown as a function of inlet-total to exit-static pressure ratio. Mass flow for the four configurations did not differ by more than 1.0 percent at any pressure ratio. However, the mass flows for both the original stator configurations are slightly larger than those for the thin stator configurations. This difference is attributed to a larger stator throat area in the original stator assembly. The difference in throat areas was due to fabrication. Choked flow conditions exist in all configurations at pressure ratios greater than 3.0.

A comparison of the efficiencies obtained with the four configurations is shown in figure 11. The maximum difference in total efficiency among the four cases was not more than two points at any pressure ratio included in the tests. The best performance, however, was obtained with the two configurations using the thin stator profiles. At design total- to static-pressure ratio, the curves for the two thin stator configurations show an efficiency of about 0.94 as compared with about 0.93 for the original stator configurations. From these results it is apparent that there was very little change in turbine performance when the stator and rotor blades were thinned by altering the pressure surface of the blade. The reason for the slight improvement in performance when using the thin stator blades is not known at this time. As indicated previously, suction-surface diffusion was the same for both stator configurations. The only difference was in pressure-surface diffusion. The thin blade configuration had considerably higher diffusion (table II) than the original blade. However, it is felt that this would have little, if any, effect on blade performance.

The curves showing the variation of static efficiency with inlet-total to exit-static-pressure ratio (fig. 11) agree very well with those presented for total efficiency, in that there was little change in performance for all configurations investigated. The maximum difference in static efficiency among the four configurations is not more than 1.5 points over the entire range of pressure ratios. At design total- to static-pressure ratio, the static efficiency for the two thin stator blade configurations is about 0.81. The curves show a value of 0.80 for the other two cases at the same pressure ratio. Table IV lists the pertinent performance values at equivalent design speed and pressure ratio for the four configurations.

It is believed that the small differences in performance are actual because the same instrumentation was used for all tests and several configurations were rerun to insure reproducibility of test results. Table II shows a slight difference in tip clearance between rotor configurations. The tip clearance for the thin rotor was 0.0051 centimeter (0.002 in.) smaller than that for the original blade. This difference would amount to about 0.3 percent change in turbine work or about 0.3 of a point in total efficiency.

Internal Flow Characteristics

A description of the internal flow characteristics is based on measured stator-exit static pressures and a rotor-exit radial survey of total pressure and flow angle.

The variation in tip static pressure with axial station for operation at design pressure ratio is shown in figure 12. Curves are presented for experimental results obtained with each of the four blade configurations, together with the design curve. It is apparent that the stator-exit static pressure was practically the same for all cases. The throat areas of the two rotors differed very little. However, the throat area of the thin stator was smaller than that of the original stator. These different stator throat areas would be conducive to unequal stator-exit static pressures. The equality of these pressures in the tests is attributed to small differences in weight flow and losses. Since the stator-exit static pressure was practically the same for all cases, the small differences in efficiencies cannot be attributed to differences in rotor reaction.

The results of rotor exit radial surveys of total pressure for the four configurations at design pressure ratio are shown in figure 13(a). The design value is also shown on the figure. Values of total pressure for the four cases are greater than design over the greater part of the blade height and do not differ by more than 2 percent. However, in all cases the pressure drops sharply near the tip to widely separated values much lower than design. This drop in total pressure is greatest for the two configurations with the thin rotor blade.

The radial variation of rotor exit flow angle at design pressure ratio is presented in figure 13(b) Design values at the hub, mean, and tip sections are also shown. The experimental values for the four configurations show similar trends over the greater part of the blade height and do not differ by more than about 5.0° from the design values. In some radial positions there is overturning of the flow; in others there is underturning.

CONCLUDING REMARKS

Results of the investigation have indicated that a substantial reduction in both stator and rotor blade thickness from the design case can be made without a penalty in turbine performance if the blade pressure surface is altered to obtain the reduction in thickness. The results indicated that there was a slight improvement in both total and static efficiencies of about 1 point when the thin stator was used with either the original or thin-rotor configuration. Comparison of blade-surface diffusion showed that the suction-surface diffusion was the same for both stator configurations. The pressure-surface diffusion was considerably higher for the thin blades than that for the original blades. This higher pressure surface diffusion apparently did not result in any penalty in blade performance. Additional tests will be required to determine the cause of the apparent increase in turbine efficiency with the thin stator blades.

Lewis Research Center,
National Aeronautics and Space Administration,
Cleveland, Ohio, October 13, 1972,
501-24.

REFERENCES

1. Cummings, Robert L.; and Gold, Harold: Concepts for Cost Reduction on Turbine Engines for General Aviation. NASA TM X-52951, 1971.

2. Kofskey, Milton G.; and Nusbaum, William J.: Design and Cold-Air Investigation of a Turbine for a Small Low-Cost Turbofan Engine. NASA TN D-6967, 1972.

3. Stewart, Warner L.: A Study of Axial-Flow Turbine Efficiency Characteristics in Terms of Velocity Diagram Parameters. Paper 61-WA-37, ASME, Dec. 1961.

4. Miser, James W.; Stewart, Warner L.; and Whitney, Warren J.: Analysis of Turbomachine Viscous Losses Affected by Changes in Blade Geometry. NACA RM E56F21, 1956.

5. Katsanis, Theodore: Fortran Program for Calculating Transonic Velocities on a Blade-to-Blade Stream Surface of a Turbomachine. NASA TN D-5427, 1969.

TABLE I. - TURBINE EQUIVALENT DESIGN VALUES

Mass flow, $\epsilon w \sqrt{\theta_{cr}}/\delta$, kg/sec; lb/sec	1.989; 4.385
Specific work, $\Delta h/\theta_{cr}$, J/g; Btu/lb	45.834; 19.690
Torque, $\tau\epsilon/\delta$, N-m; ft-lb	56.727; 41.840
Rotative speed, $N/\sqrt{\theta_{cr}}$, rpm	15 336
Rotor mean section blade speed, $U_m/\sqrt{\theta_{cr}}$, m/sec; ft/sec	163.17; 535.33
Total- to static-pressure ratio, p_1'/p_3	2.298
Total- to total-pressure ratio, p_1'/p_3'	2.018
Blade-jet speed ratio, ν	0.466
Work-speed parameter, λ	0.582

TABLE II. - TURBINE AERODYNAMIC PARAMETERS

Turbine blading	Blade row	Section	Blade-surface diffusion parameter[a]		Blade turning, deg	Blade chord		Solidity	Reaction[a]	Aspect ratio[b]	Number of blades	Tip clearance	
			Suction surface, D_s	Pressure surface, D_p		cm	in.					cm	in.
Original profile	Stator	Tip	1.232	1.241	68.7	2.946	1.160	1.39	0.873				
		Mean	1.233	1.309	65.0	2.616	1.030	1.43	.900	1.29	35	-----	-----
		Hub	1.284	1.032	61.5	2.400	.945	1.35	.927				
	Rotor	Tip	1.302	1.892	63.9	2.654	1.045	1.50	0.855				
		Mean	1.180	2.176	91.2	2.606	1.026	1.71	.778	1.39	42	0.030	0.012
		Hub	1.213	2.267	111.0	2.758	1.086	2.18	.512				
Thin profile	Stator	Tip	1.232	5.635	68.7	2.946	1.160	1.39	0.873				
		Mean	1.233	5.531	65.0	2.616	1.030	1.43	.900	1.29	35	-----	-----
		Hub	1.284	5.742	61.5	2.400	.945	1.35	.927				
	Rotor	Tip	1.302	4.223	63.9	2.654	1.045	1.50	0.855				
		Mean	1.180	6.108	91.2	2.606	1.026	1.71	.778	1.39	42	0.025	0.010
		Hub	1.213	8.675	111.0	2.758	1.086	2.18	.512				

[a]See section SYMBOLS for definition.

[b]Based on average blade height and mean chord.

TABLE III. - BLADE SECTION COORDINATES

[Trailing-edge radius, 0.025 cm; all coordinate dimensions are in cm.]

(a) Stator; leading-edge radius, 0.127 centimeter

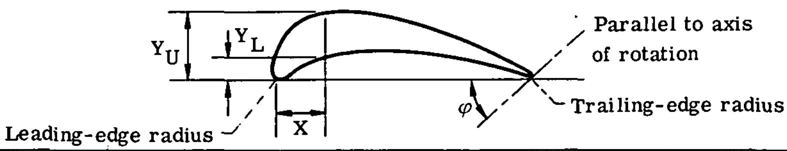

X	Original blade profile						Thin blade profile					
	Hub		Mean		Tip		Hub		Mean		Tip	
	Radius, r, cm											
	8.479		10.160		11.844		8.479		10.160		11.844	
	Orientation angle, φ, deg											
	43.65		43.03		39.97		43.65		43.03		39.97	
	Y_U	Y_L	Y_U	Y_L	Y_U	Y_L	Y_U	Y_L	Y_U	Y_L	Y_U	Y_L
0.000	0.127	0.127	0.127	0.127	0.127	0.127	0.127	0.127	0.127	0.127	0.127	0.127
.127	.445	.000	.424	.000	.427	.000	.445	.000	.424	.000	.427	.000
.254	.559	.056	.538	.043	.549	.036	.559	.109	.538	.109	.549	.109
.381	.615	.119	.599	.094	.625	.081	.615	.340	.599	.315	.625	.323
.508	.643	.173	.632	.135	.671	.124	.643	.386	.632	.373	.671	.404
.635	.653	.211	.650	.170	.696	.160	.653	.401	.650	.394	.696	.437
.762	.648	.241	.653	.198	.706	.191	.648	.404	.653	.399	.706	.452
.889	.632	.259	.648	.216	.706	.218	.632	.391	.648	.391	.706	.449
1.016	.610	.267	.632	.224	.696	.236	.610	.371	.632	.373	.696	.439
1.143	.579	.267	.612	.229	.681	.249	.579	.345	.612	.350	.681	.422
1.270	.544	.257	.584	.226	.658	.257	.544	.310	.584	.320	.658	.399
1.397	.503	.241	.549	.221	.630	.262	.503	.277	.549	.289	.630	.371
1.524	.457	.221	.511	.211	.602	.257	.457	.241	.511	.259	.602	.338
1.651	.406	.196	.467	.196	.564	.249	.406	.203	.467	.229	.564	.307
1.778	.351	.165	.422	.175	.523	.234	.351	.168	.422	.195	.523	.277
1.905	.295	.132	.373	.150	.483	.218	.295	.132	.373	.165	.483	.246
2.032	.234	.097	.320	.122	.439	.196	.234	.096	.320	.135	.439	.216
2.159	.173	.061	.264	.094	.394	.170	.173	.061	.264	.104	.394	.183
2.286	.104	.025	.203	.069	.343	.142	.104	.025	.203	.074	.343	.152
2.400	.025	.025	-----	-----	-----	-----	.025	.025	-----	-----	-----	-----
2.413	-----	-----	.145	.038	.287	.117	-----	-----	.145	.043	.287	.122
2.540	-----	-----	.084	.010	.231	.089	-----	-----	.084	.010	.231	.091
2.616	-----	-----	.025	.025	-----	-----	-----	-----	.025	.025	-----	-----
2.667	-----	-----	-----	-----	.178	.061	-----	-----	-----	-----	.178	.061
2.794	-----	-----	-----	-----	.117	.030	-----	-----	-----	-----	.117	.030
2.921	-----	-----	-----	-----	.058	.000	-----	-----	-----	-----	.056	.000
2.946	-----	-----	-----	-----	.025	.025	-----	-----	-----	-----	.025	.025

TABLE III. - Concluded. BLADE SECTION COORDINATES

[Trailing-edge radius, 0.025 cm all coordinate dimensions are in cm.]

(b) Rotor

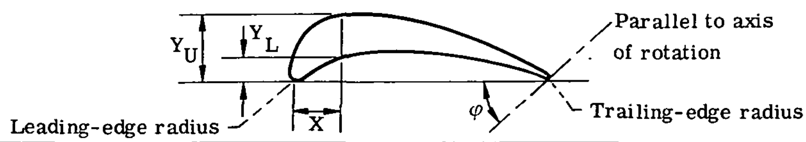

X	Original blade profile						Thin blade profile					
	Hub		Mean		Tip		Hub		Mean		Tip	
	Radius, r, cm											
	8.471		10.160		11.839		8.471		10.160		11.839	
	Orientation angle, φ, deg											
	17.07		31.05		42.00		17.07		31.05		42.00	
	Leading-edge radius, cm											
	0.097		0.081		0.064		0.097		0.081		0.064	
	Y_U	Y_L	Y_U	Y_L	Y_U	Y_L	Y_U	Y_L	Y_U	Y_L	Y_U	Y_L
0.00	0.097	0.097	0.081	0.081	0.064	0.064	0.097	0.097	0.081	0.081	0.064	0.064
.127	.396	.005	.366	.018	.312	.030	.396	.005	.366	.018	.312	.046
.254	.607	.142	.531	.112	.437	.124	.607	.229	.531	.267	.437	.262
.381	.762	.279	.632	.196	.511	.196	.762	.455	.632	.432	.511	.363
.508	.874	.389	.704	.257	.559	.244	.874	.617	.704	.526	.559	.422
.635	.955	.472	.744	.310	.587	.282	.955	.734	.744	.579	.587	.452
.762	1.011	.533	.767	.343	.599	.305	1.011	.805	.767	.604	.599	.465
.889	1.039	.574	.772	.368	.594	.318	1.039	.846	.772	.612	.594	.465
1.016	1.049	.599	.765	.381	.584	.320	1.049	.858	.765	.604	.584	.452
1.143	1.044	.615	.742	.389	.564	.315	1.044	.851	.742	.584	.564	.432
1.270	1.021	.620	.711	.381	.538	.307	1.021	.825	.711	.556	.538	.404
1.397	.988	.610	.671	.373	.508	.292	.988	.787	.671	.521	.508	.371
1.524	.940	.592	.627	.358	.470	.274	.940	.742	.627	.477	.470	.333
1.651	.884	.564	.572	.335	.432	.251	.884	.686	.572	.432	.432	.295
1.778	.818	.533	.513	.305	.391	.224	.818	.620	.513	.383	.391	.254
1.905	.744	.493	.450	.267	.348	.193	.744	.551	.450	.330	.348	.216
2.032	.655	.437	.386	.226	.302	.163	.655	.475	.386	.272	.302	.178
2.159	.561	.373	.320	.180	.254	.130	.561	.394	.320	.213	.254	.140
2.286	.462	.302	.251	.127	.206	.097	.462	.310	.251	.152	.206	.102
2.413	.358	.224	.170	.071	.152	.056	.358	.226	.170	.086	.152	.064
2.540	.246	.137	.086	.013	.097	.025	.246	.137	.086	.020	.097	.025
2.606	-----	-----	.025	.025	-----	-----	-----	-----	.025	.025	-----	-----
2.654	-----	-----	-----	-----	.025	.025	-----	-----	-----	-----	.025	.025
2.667	.127	.046	-----	-----	-----	-----	.127	.046	-----	-----	-----	-----
2.758	.025	.025	-----	-----	-----	-----	.025	.025	-----	-----	-----	-----

TABLE IV. - EXPERIMENTAL PERFORMANCE VALUES

Configuration	Efficiency		Equivalent specific work, $\Delta h/\theta_{cr}$		Equivalent mass flow, $\epsilon w\sqrt{\theta_{cr}}/\delta$		Equivalent torque, $\tau\epsilon/\delta$	
	Total, η_t	Static, η_s	J/g	Btu/lb	kg/sec	lb/sec	N-m	ft-lb
Original stator, original rotor	0.93	0.80	49.3	21.2	2.00	4.41	61.3	45.2
Original stator, thin rotor	0.93	0.80	49.2	21.1	1.99	4.38	60.7	44.8
Thin stator, original rotor	0.94	0.81	49.9	21.4	1.98	4.37	61.6	45.4
Thin stator, thin rotor	0.94	0.81	50.1	21.5	1.98	4.37	61.6	45.4

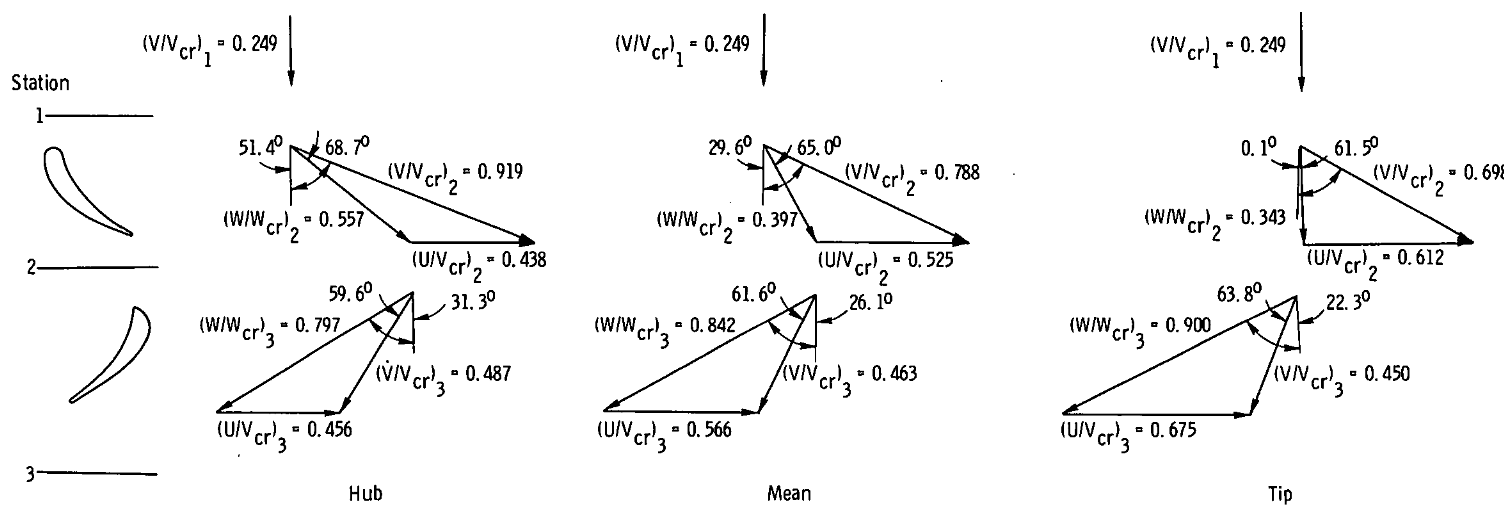

Figure 1. - Design free-stream velocity diagrams.

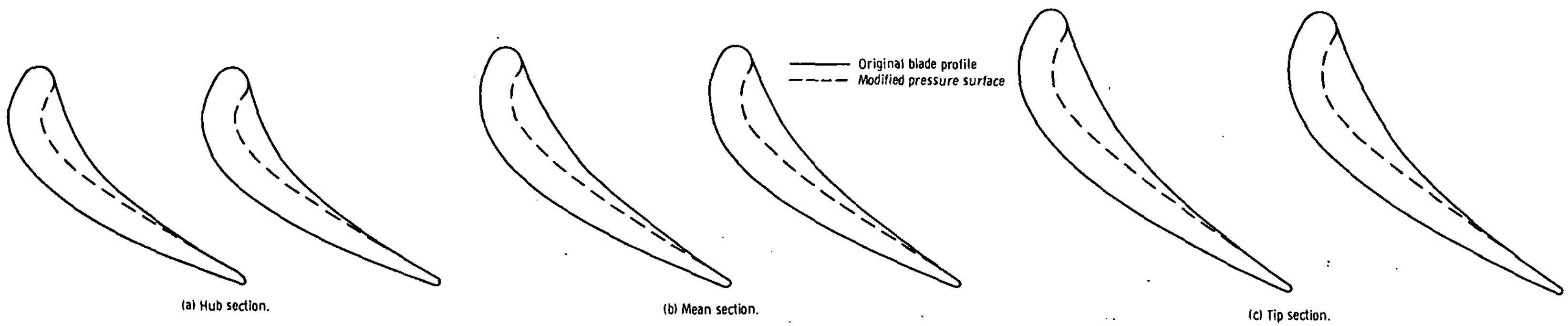

Figure 2. - Stator-blade profiles and passages.

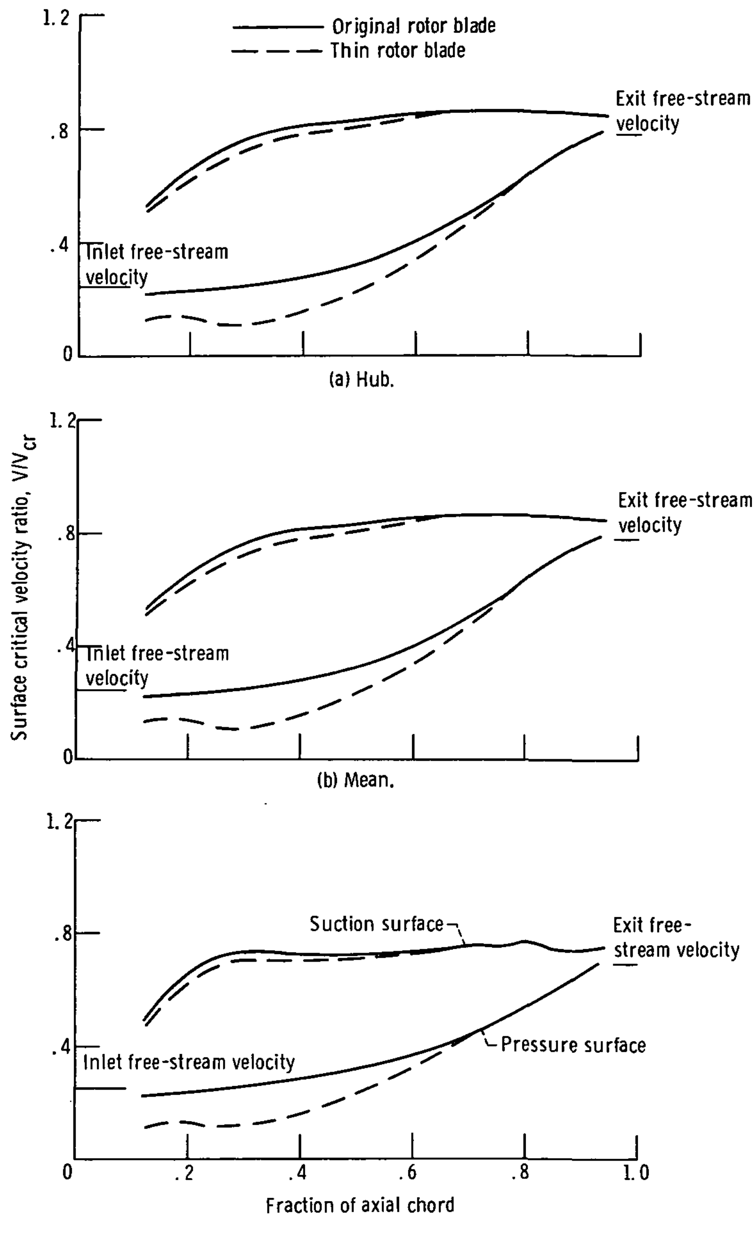

Figure 3. - Design stator-blade surface velocities.

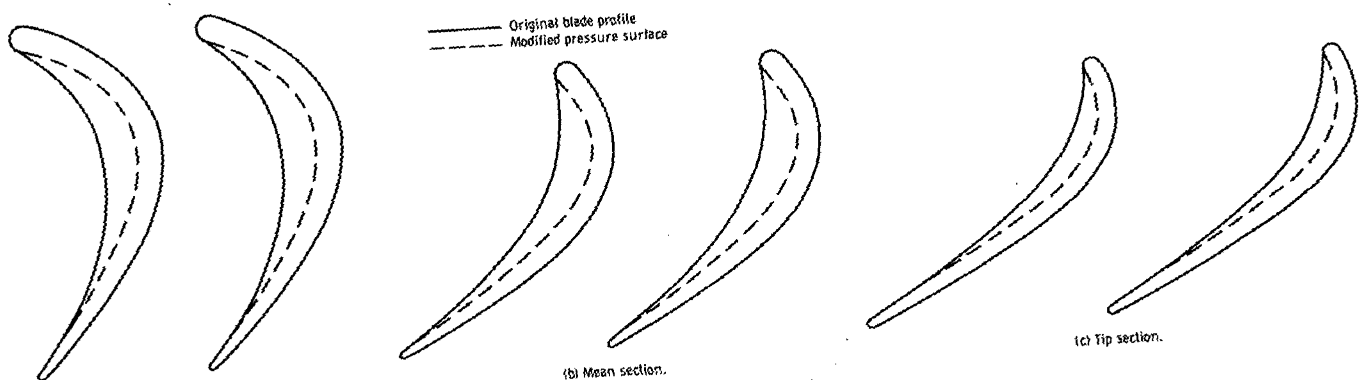

(a) Hub section.

(b) Mean section.

(c) Tip section.

Figure 4. - Rotor-blade profiles and passages.

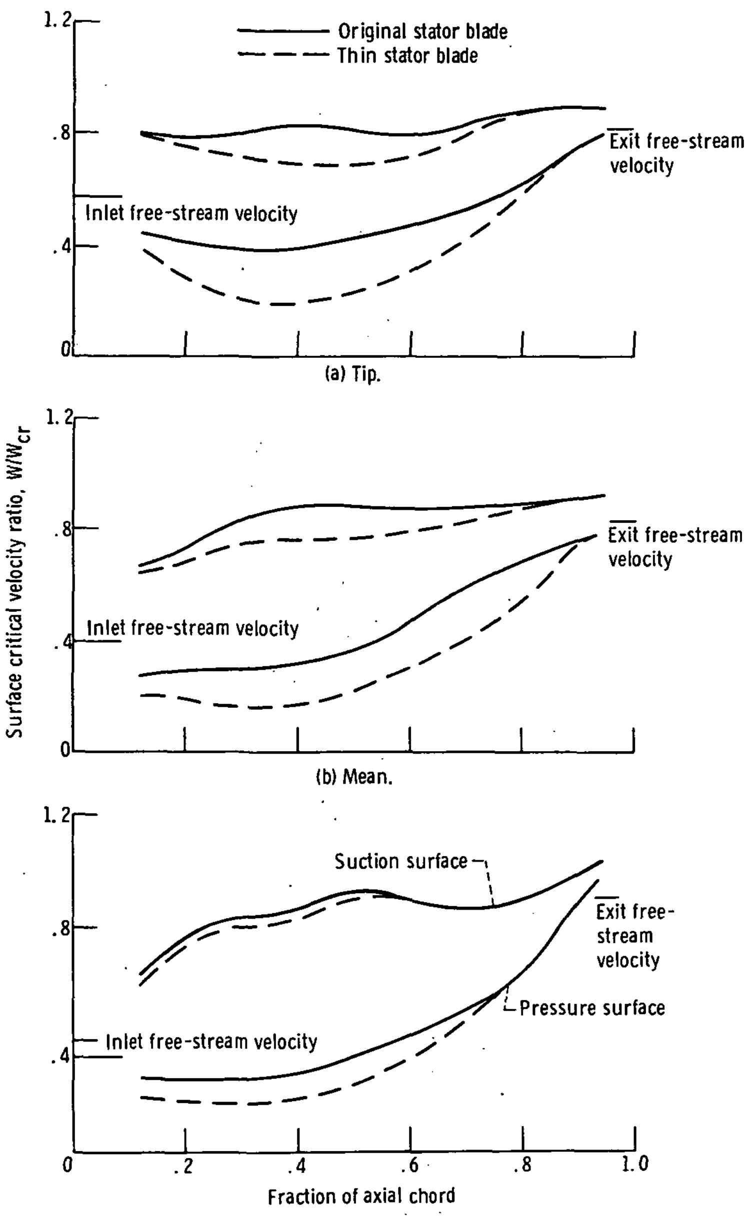

Figure 5. - Design rotor-blade surface velocities.

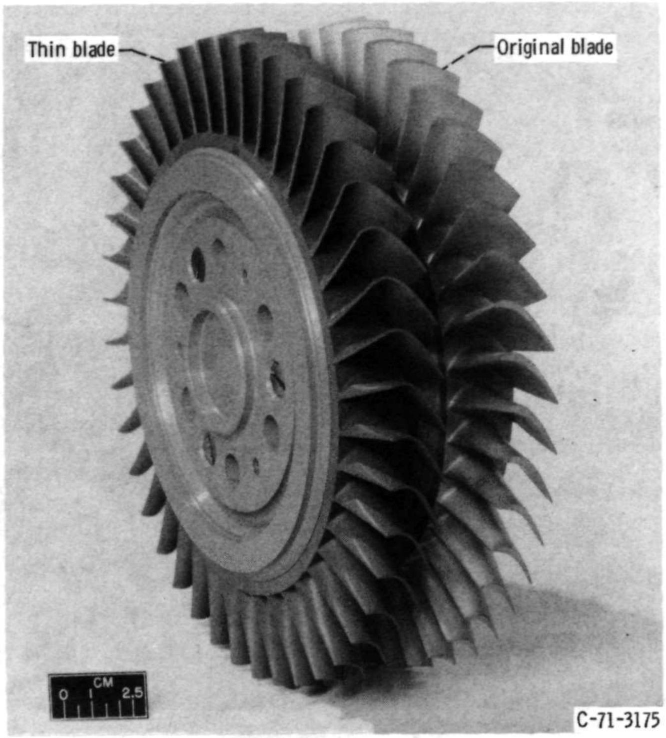

Figure 6. - Rotor-blade configurations investigated.

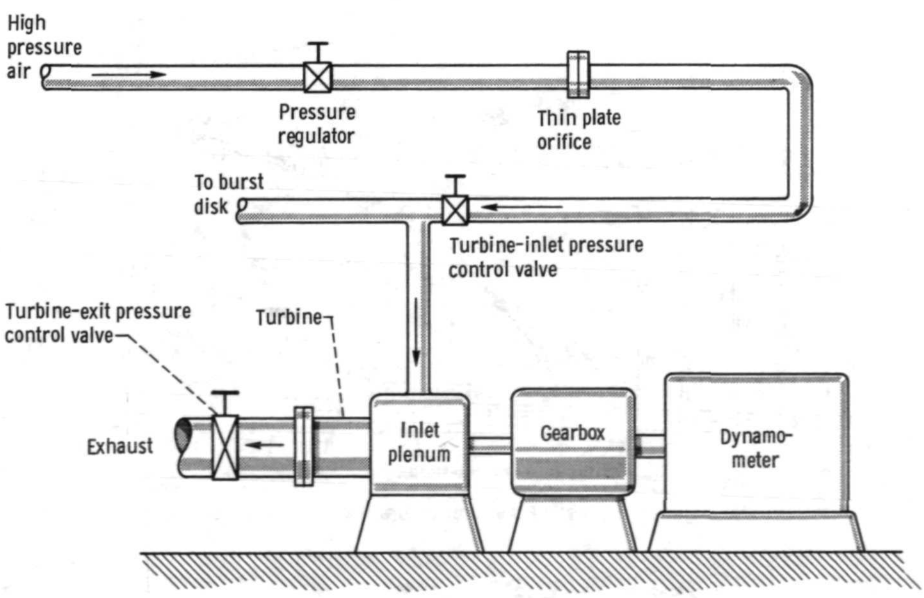

Figure 7. - Experimental equipment.

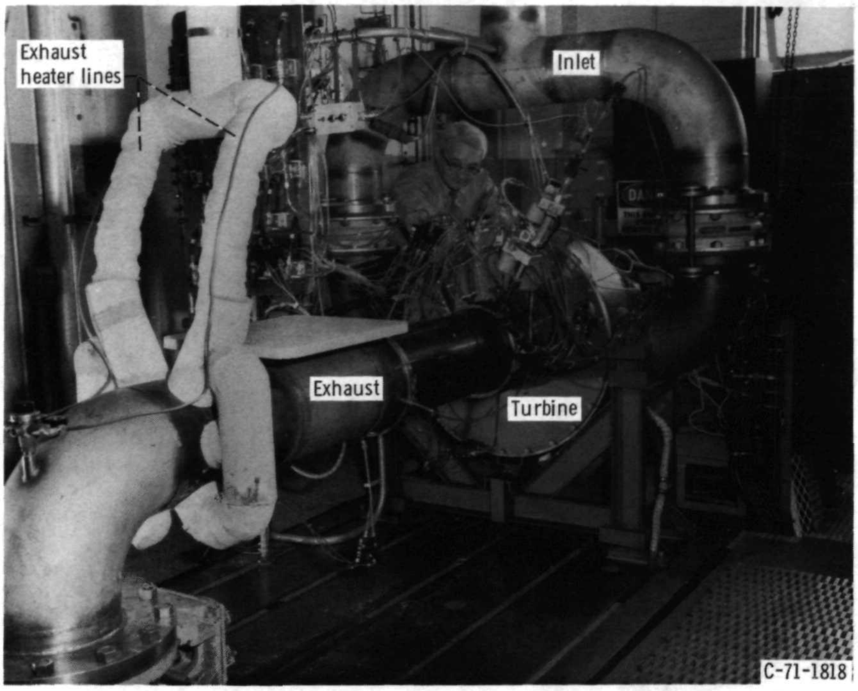

Figure 8. - Turbine test apparatus.

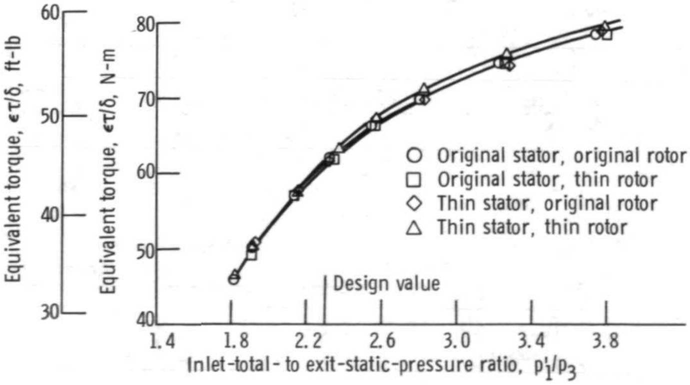

Figure 9. - Variation of equivalent torque at equivalent design speed.

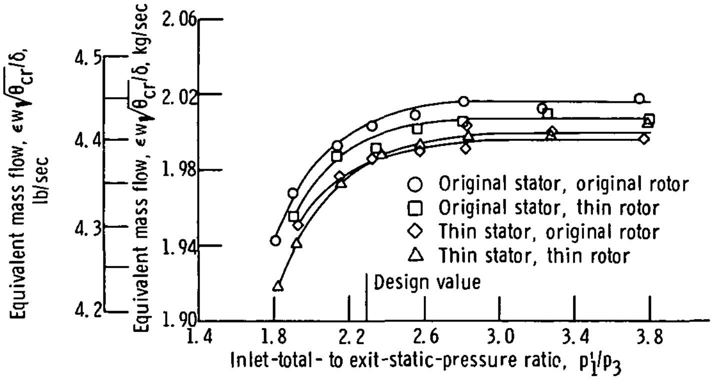

Figure 10. - Variation of equivalent mass flow at equivalent design speed.

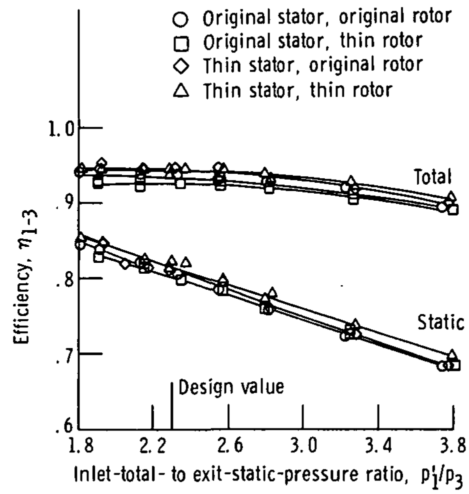

Figure 11. - Variation of efficiency at equivalent design speed.

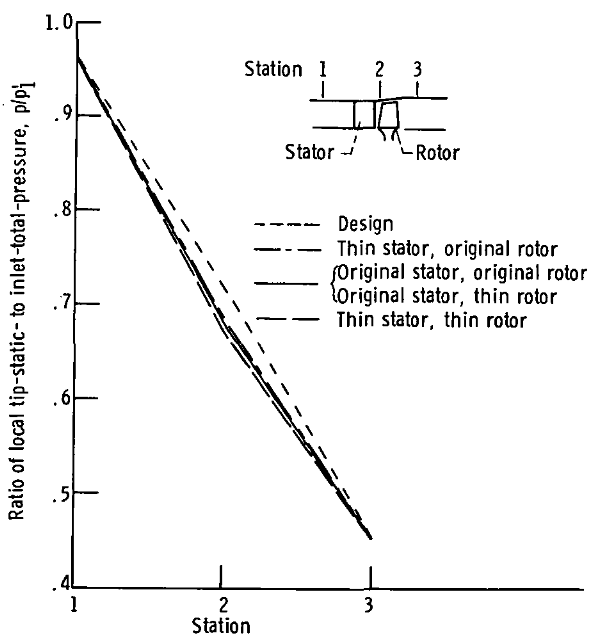

Figure 12. - Variation of tip static pressure with axial station at equivalent design speed and design total- to static-pressure ratio.

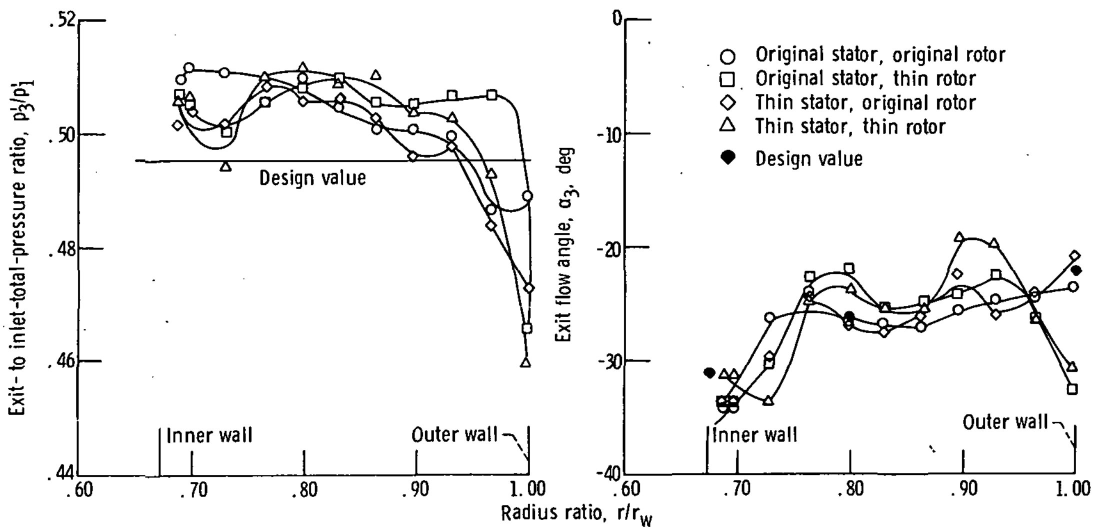

(a) Exit total pressure.

(b) Exit flow angle.

Figure 13. - Variation of rotor-exit total pressure and flow angle with radius ratio at equivalent design speed and pressure ratio.

NASA-Langley, 1973 —— 28 E-7029

"The aeronautical and space activities of the United States shall be conducted so as to contribute . . . to the expansion of human knowledge of phenomena in the atmosphere and space. The Administration shall provide for the widest practicable and appropriate dissemination of information concerning its activities and the results thereof."

—NATIONAL AERONAUTICS AND SPACE ACT OF 1958

NASA SCIENTIFIC AND TECHNICAL PUBLICATIONS

TECHNICAL REPORTS: Scientific and technical information considered important, complete, and a lasting contribution to existing knowledge.

TECHNICAL NOTES: Information less broad in scope but nevertheless of importance as a contribution to existing knowledge.

TECHNICAL MEMORANDUMS: Information receiving limited distribution because of preliminary data, security classification, or other reasons.

CONTRACTOR REPORTS: Scientific and technical information generated under a NASA contract or grant and considered an important contribution to existing knowledge.

TECHNICAL TRANSLATIONS: Information published in a foreign language considered to merit NASA distribution in English.

SPECIAL PUBLICATIONS: Information derived from or of value to NASA activities. Publications include conference proceedings, monographs, data compilations, handbooks, sourcebooks, and special bibliographies.

TECHNOLOGY UTILIZATION PUBLICATIONS: Information on technology used by NASA that may be of particular interest in commercial and other non-aerospace applications. Publications include Tech Briefs, Technology Utilization Reports and Technology Surveys.

Details on the availability of these publications may be obtained from:

SCIENTIFIC AND TECHNICAL INFORMATION OFFICE

NATIONAL AERONAUTICS AND SPACE ADMINISTRATION

Washington, D.C. 20546